

Supporting Information

Soluble, Optically Transparent Polyamides with Phosphaphenanthrene Skeleton: Synthesis, Characterization, Gas Permeation and Molecular Dynamics Simulations

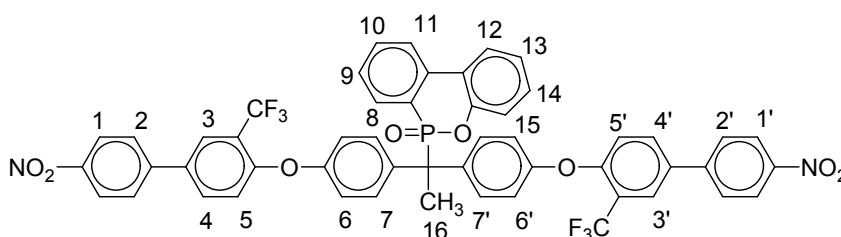
Soumendu Bisoi^a, Arun Kumar Mandal^a, Asheesh Singh^a, Venkat Padmanabhan^b,
Susanta Banerjee^{a*}

^aMaterials Science Centre, Indian Institute of Technology Kharagpur,
Kharagpur - 721302, India

^bDepartment of Chemical Engineering, Tennessee Technological University, Cookeville,
TN 38505, USA

Synthesis of monomers

Synthesis of the dinitro compound (iii)

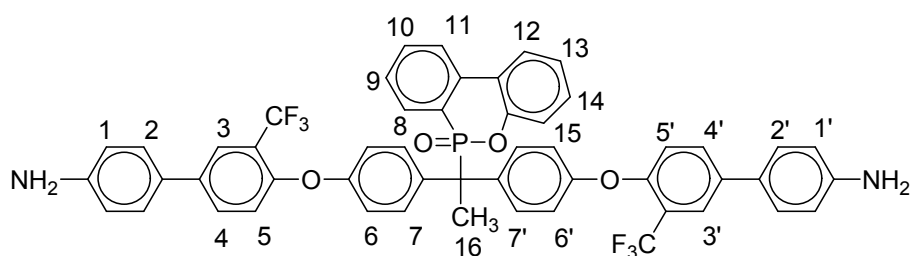


In a 100 mL round bottom flask equipped with a nitrogen inlet a condenser and a magnetic stirrer, 1,1-bis(4-hydroxyphenyl)-1-(6-oxido-6H-dibenz<c,e><1,2>oxaphosphorin-6-yl)ethane (6.0 g, 14.0 mmol), 4-fluoro-4'-nitro-3-trifluoromethyl-biphenyl (8.38 g, 29.41 mmol), K₂CO₃ (3.90 g, 28.24 mmol) and dry DMAc (50 mL) were added. The reaction mixture was heated for 12 h at temperature 120 °C. Then, the reaction mixture was cooled to room temperature and was poured slowly into 500 mL ethanol/water (1/2, V/V) under stirring. The crude precipitate was filtered, washed with water for several times and dried in vacuum at 80 °C for overnight. The crude compound was purified by silica gel column chromatography using hexane/ethyl acetate as eluent to obtain pure dinitro compound (iii). Yield: 11.14 g, (83 %).

Anal. calcd for C₅₂H₃₃F₆N₂O₈P (958.79 g mol⁻¹): C, 65.14 %; H, 3.47 %; F, 11.89 %; N, 2.92 %, O, 13.35 %; P, 3.23 %. %; found: C, 65.11 %; H, 3.52 %; F, 11.93 %; N,

2.90 %; O, 13.33 %; P, 3.24 %. $^1\text{H-NMR}$: $^1\text{H-NMR}$: $\delta_{\text{H(ppm)}}$ (600 MHz; CDCl_3 ; Me_4Si): δ 8.33 (d, $J = 8.7$ Hz, 4H), 8.14 (q, $J = 11.5, 10.0$ Hz, 5H, H2, H2', H5), 8.07 - 8.04 (m, 5H, H3, H3', H8, H11, H12), 7.77 (t, 1H, H4), 7.50 - 7.46 (m, 3H, H5, H5', H14), 7.40 - 7.38 (m, 4H, H7, H7'), 7.26 (t, 1H, H13), 7.20 (d, $J = 8.1$ Hz, 1H, H15), 7.08 - 6.97 (m, 6H, H4, H4', H6, H6'), 1.82 (d, $J = 16.5$ Hz, 3H).

Synthesis of the diamine monomer (4)



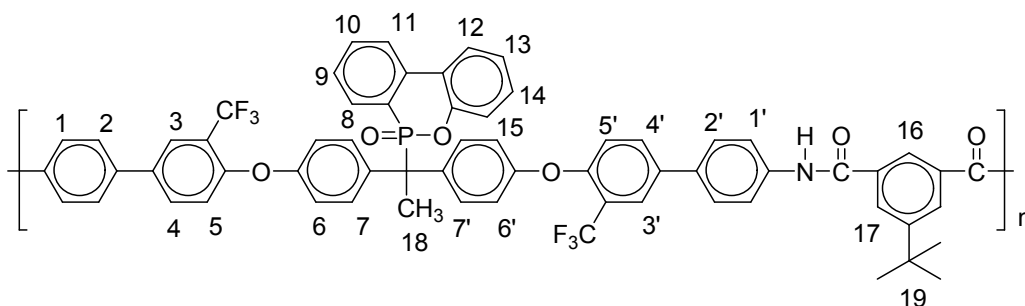
The dinitro compound (iii) (8.7 g, 9.07 mmol), Pd-C (Pd content 1%, 0.32 g), and THF (90 mL) were taken in a three-necked round bottom flask equipped with a stirring bar, dropping funnel and condenser. Hydrazine monohydrate (60 mL) was added drop wise over a period of 1 h at 80 °C to this mixture. The mixture was heated to reflux for 48 h under N_2 atmosphere. After this period, the reaction mixture was filtered to remove Pd/C and excess solvent was distilled off from the reaction mixture. The remaining solvent was poured into 500 mL of water under stirring. The precipitate was filtered and then dried in a vacuum oven at 50 °C. The crude precipitate was purified by column chromatography using dichloromethane as an eluent to obtain pure diamine compound (4). Yield: 7.01 g, (86 %).

Anal. calcd for $\text{C}_{52}\text{H}_{37}\text{F}_6\text{N}_2\text{O}_4\text{P}$ (898.83 g mol^{-1}): C, 69.49 %; H, 4.15 %; F, 12.68 %; N, 3.12 %; O, 7.12 %; P, 3.45 %. %; found: C, 69.47 %; H, 4.16 %; F, 12.71 %; N, 3.11 %; O, 7.08 %; P, 3.41 %. $^1\text{H-NMR}$: $\delta_{\text{H(ppm)}}$ (600 MHz, DMSO-d_6 ; Me_4Si): δ 8.15 (t, 1H, H8), 8.04 (d, $J = 7.6$ Hz, 1H, H12), 7.89 - 7.81 (m, 4H, H3, H3', H9, H10), 7.75 (t, $J = 7.7$ Hz, 1H, H14), 7.45 - 7.39 (m, 7H, H4, H4', H7, H7', H11), 7.34 (d, $J = 7.4$ Hz, 4H,

H6, H6'), 7.23 (t, 1H, H13), 7.19 (d, $J = 8.1$ Hz, 1H, H15), 6.98 (t, 2H, H5, H5'), 6.89 (t, 4H, H2, H2'), 6.68 (d, $J = 8.5$ Hz, 4H, H1, H1'), 5.34 (s, 2H, amine protons), 1.77 (d, $J = 16.7$ Hz, 3H, H16).

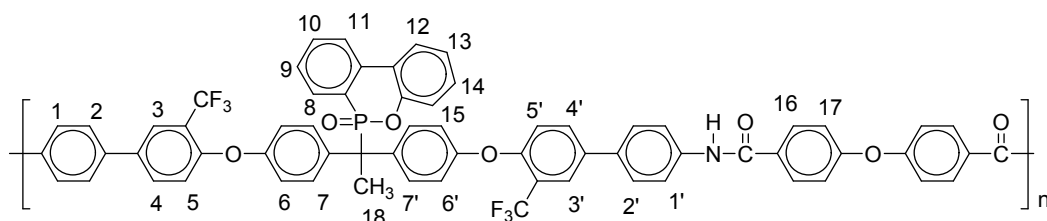
Characterization of the polymers

PA 4A



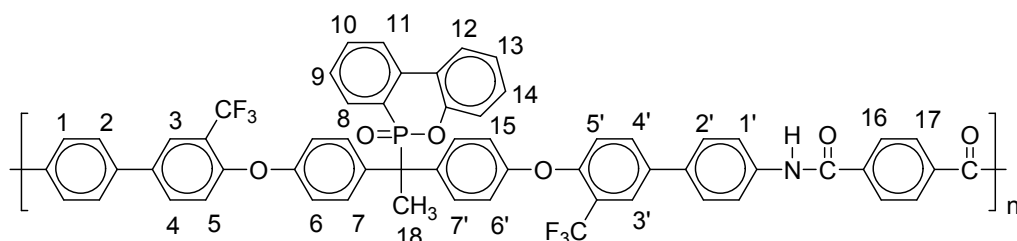
Anal. calcd for $C_{64}H_{47}F_6N_2O_6P$ (1085.03 g mol⁻¹): C, 69.69 %; H, 4.48 %; F, 10.33 %; N, 2.54 %; O, 10.15 %; P, 2.81 %. %; found: C, 69.74 %; H, 4.51 %; F, 10.31 %; N, 2.52 %; O, 10.18 %, P, 2.78 %. FTIR (KBr, cm⁻¹): 3322 (N-H stretching), 1664 (>C=O stretching), 920 (P-O-Ph stretching). ¹H-NMR: $\delta_{H(ppm)}$ (600 MHz; Pyridine-d₅; Me₄Si): δ 11.54 (s, 2H, amide protons), 9.09 (s, 1H, H16), 8.49 (s, 2H, H17), 8.36 (s, 4H, H1, H1'), 8.11 (d, $J = 8.4$ Hz, 2H, H3, H3'), 8.05 (s, 1H, H11), 8.00 (d, $J = 7.9$ Hz, 1H, H12), 7.94 (d, $J = 12$ Hz, 1H, H8), 7.81 (d, $J = 12$ Hz, 1H, H10), 7.71 (m, 8H, H7, H7', H2, H2'), 7.66 (d, $J = 7.8$ Hz, 2H, H4, H4'), 7.59 (t, 1H, H9), 7.41 (m, 1H, H15), 7.36 (s, 1H, H13), 7.22 (s, 4H, H6, H6'), 7.11 (m, 7H, H2, H5, H14), 2.05 (d, $J = 16.3$ Hz, 3H, H18), 1.16 (s, 9H, H19).

PA 4B



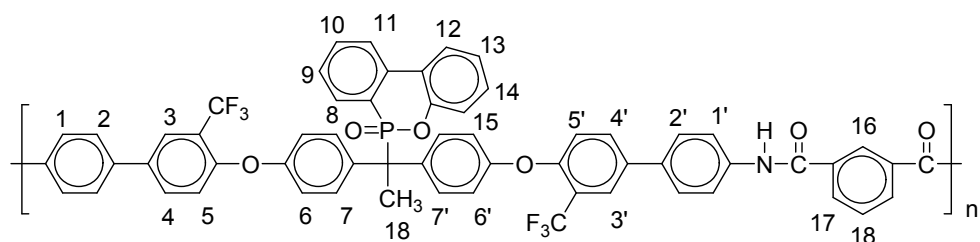
Anal. calcd for $C_{66}H_{43}F_6N_2O_7P$ (1121.02 g mol⁻¹): C, 70.71 %; H, 3.87 %; F, 10.17 %; N, 2.50 %; O, 9.99 %; P, 2.76 %. %; found: C, 69.74 %; H, 4.51 %; F, 10.14 %; N, 2.52 %; O, 9.95 %, P, 10.16 %. FTIR (KBr, cm⁻¹): 3353 (N-H stretching), 1652 (>C=O stretching), 1230 (P=O stretching), 915 (P-O-Ph stretching). ¹H-NMR: $\delta_{H(ppm)}$ (600 MHz; Pyridine-d₅; Me₄Si): δ 11.25 (s, 2H, amide protons), 8.39 - 8.36 (m, 8H, H1, H1', H16), 8.11 (d, $J = 8.3$ Hz, 2H, H3, H3'), 8.05 (s, 2H, H12), 8.00 (d, $J = 7.9$ Hz, 2H, H15), 7.92 (d, $J = 8.3$ Hz, 2H, H13), 7.89 (d, $J = 8.4$ Hz, 2H, H11), 7.81 (m, 6H, H17, H4), 7.71 (d, $J = 8.0$ Hz, 2H, H5, H5'), 7.66 (s, 1H, H14), 7.41 (m, 1H, H10), 7.36 (m, 1H, H8), 7.26 (m, 1H, H9), 7.17 (s, 6H, H7), 7.11 - 7.09 (m, 12H, H2, H2', H6, H6', H7, H7'), 2.05 (d, $J = 16.3$ Hz, 3H, H18).

PA 4C



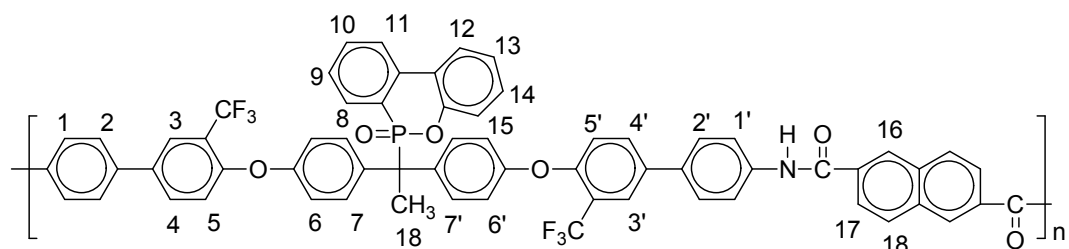
Anal. calcd for $C_{60}H_{39}F_6N_2O_6P$ (1028.93 g mol⁻¹): C, 70.04 %; H, 3.82 %; F, 11.08 %; N, 2.72 %; O, 9.33 %; P, 3.01 %. %; found: C, 70.01 %; H, 3.83 %; F, 11.11 %; N, 2.68 %; O, 9.34 %; P, 3.03 %. FTIR (KBr, cm⁻¹): 3360 (N-H stretching), 1654 (>C=O stretching), 1232 (P=O stretching), 919 (P-O-Ph stretching). ¹H-NMR: $\delta_{H(ppm)}$ (600 MHz; Pyridine-d₅; Me₄Si): δ 11.38 (s, 2H, amide protons), 8.42 (s, 2H, 16H), 8.32 (s, 2H, H17), 8.10 - 8.00 (m, 5H, H7, H7', H12), 7.88 (m, 2H, H3, H3'), 7.80 (m, 6H, H1, H1', H14, H15), 7.71 (m, 2H, H13, H8), 7.66 (s, 1H, H11), 7.38 (d, $J = 35.3$ Hz, 3H, H5, H5', H14), 7.23 (m, 5H, H6, H6', H8), 7.12 (m, 6H, H2, H2', H9, H10), 2.04 (s, 3H, H18).

PA 4D



Anal. calcd for $C_{60}H_{39}F_6N_2O_6P$ (1028.93 g mol⁻¹): C, 70.04 %; H, 3.82 %; F, 11.08 %; N, 2.72 %; O, 9.33 %; P, 3.01 %. %; found: C, 70.02 %; H, 3.83 %; F, 11.09 %; N, 2.69 %; O, 9.36 %; P, 3.02 %. FTIR (KBr, cm⁻¹): 3362 (N-H stretching), 1664 (>C=O stretching), 1236 (P=O stretching), 919 (P-O-Ph stretching). ¹H-NMR: $\delta_{H(ppm)}$ (600 MHz; Pyridine-d₅; Me₄Si): δ 11.35 (s, 2H, amide protons), 9.14 (s, 1H, H16), 8.38 (d, $J = 18$ Hz, 2H, H17), 8.29 (m, 4H, H7, H7'), 8.08 (d, $J = 8.4$ Hz, 2H, H3, H3'), 8.02 (m, 2H, H4), 7.97 (d, $J = 7.9$ Hz, 1H, H12), 7.89 (m, 1H, H15), 7.86 (m, 1H, H18), 7.71 (d, $J = 18$ Hz, 4H, H2, H2'), 7.78 (m, 6H, H1, H1', H5, H5'), 7.55 (s, 1H, H13), 7.49 (s, 1H, H11), 7.38 (s, 1H, H14), 7.18-7.10 (m, 5H, H6, H6', H10), 7.09 - 7.05 (m, 2H, H8, H9), 2.02 (d, $J = 12$ Hz, 3H, H19).

PA 4E



Anal. calcd for $C_{64}H_{41}F_6N_2O_6P$ (1078.98 g mol⁻¹): C, 71.24 %; H, 3.83 %; F, 10.56 %; N, 2.60 %; O, 8.90 %; P, 2.87 %. %; found: C, 71.27 %; H, 3.86 %; F, 10.53 %; N, 2.62 %; O, 8.92 %; P, 2.88 %. FTIR (KBr, cm⁻¹): 3352 (N-H stretching), 1664 (>C=O

stretching), 1232 (P=O stretching), 915 (P-O-Ph stretching). ¹H-NMR: δ_{H(ppm)} (600 MHz; Pyridine-d₅; Me₄Si): δ 11.46 (s, 2H, amide protons), 8.84 (s, 2H), 8.42 (m, 6H, H3, H17, H18), 8.13 (d, *J* = 7.9 Hz, 2H, H4, H4'), 8.05 (m, 1H, H12), 8.00 (m, 4H, H1, H1'), 7.95 (d, *J* = 6 Hz, 1H, H15), 7.95 (d, *J* = 12 Hz, 1H, H13), 7.84 (m, 5H, H2, H2', H14), 7.72 (d, *J* = 7.6 Hz, 2H, H5, H5'), 7.66 (m, 1H, H11), 7.41 (m, 1H, H10), 7.36 (m, 1H, H8), 7.22 (s, 4H, H7, H7'), 7.14 - 7.10 (m, 5H, H9, H6, H6'), 2.03 (d, *J* = 12.6 Hz, 3H, H19).

Film quality, color and dielectric constant

The solution cast membranes were colorless and transparent. All PAs membranes showed foldable property. **Fig. S1** shows the pictures of our PA membranes and analogous polyamide membranes from previous work with reference to Kapton.¹ It can be clearly seen from the photographs that incorporation of the bulky phenolphthalein anilide group in the polymer backbone of PEA IV reduces its color intensity in comparison to PEA I membrane. PEA IV has higher FFV (0.254) in comparison to PEA I (FFV ~ 0.188).¹ When we compared the color of PA 4A (FFV~0.298) membrane from this investigation with analogous PEA IV (FFV~ 0.254), it is found that there is a drastic reduction in color of this membrane. Thus, phosphaphenanthrene skeleton in the PAs backbone helped in reduction in color of the PA membranes. In general all the PA membranes in this investigation showed very low color intensity in comparison to as prepared Kapton[®] type of film in laboratories by the reaction of PMDA and ODPA.

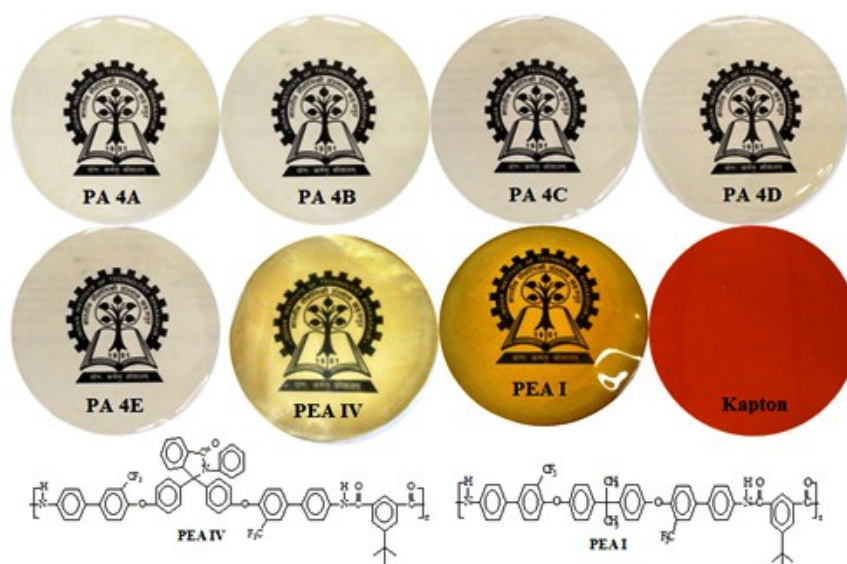


Fig. S1. The photograph of the PA membranes from this investigation and from our previous work¹ reference to Kapton type film.

Molecular packing

The **Fig. S2** exhibits WAXD patterns of the PA membranes, as a function of 2θ ($^\circ$). The interchain packing of the polymer membranes was investigated from the WAXD measurements. The polymer membranes were exhibited typical broad and structure less curves suggesting that all polymers are amorphous in nature.² This is due to the presence of bulky phosphaphenanthrene skeleton in polymer backbone which hindered the extent of close packing of polymer chains.³ In the WAXD pattern, the position of the halo maximum can be considered as an indicator of the most probable intersegmental distance (d_{sp}) between the chains. The position and shape of amorphous halo were dependent on diacid monomers. All PA membranes had two broad diffraction peaks, ranging from low angel side to high angel side. For PA 4A, PA 4B, PA 4D and PA 4E peaks located at low angel $2\theta = 12.13^\circ, 12.9^\circ, 12.2$ and 14.3° can be assigned to the main inter chain distance in the amorphous domain. For PA 4A, PA 4B, PA 4C, PA 4D and PA 4E peaks located at high angel side $2\theta = 19.5^\circ, 19.3^\circ, 21.1, 21.3$ and 21.4° can be assigned to the π - π stacking of aromatic rings or the interchain distance in the ordered domain or the lose stacks in the

polymer chains. Different diffraction pattern in WAXD provides the different free volume morphologies, which affects FFV and gas permeability of the polymers.

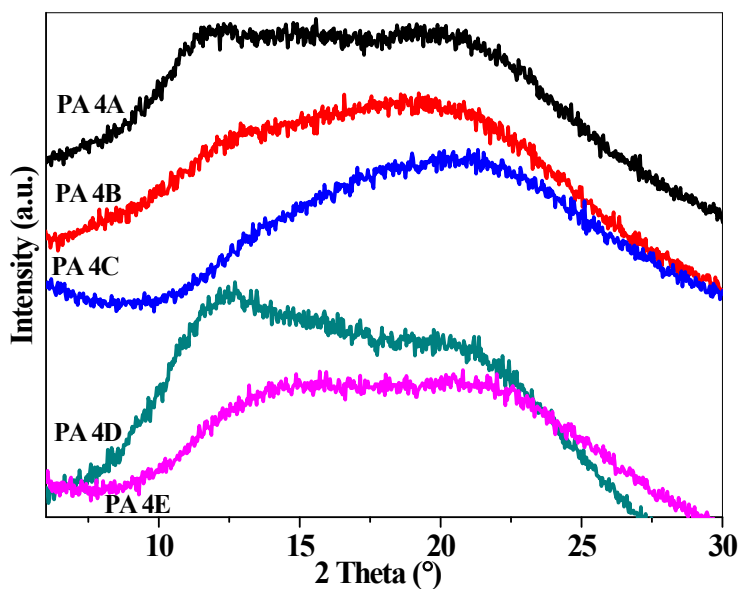


Fig. S2. WAXD patterns of the polyamide membranes.

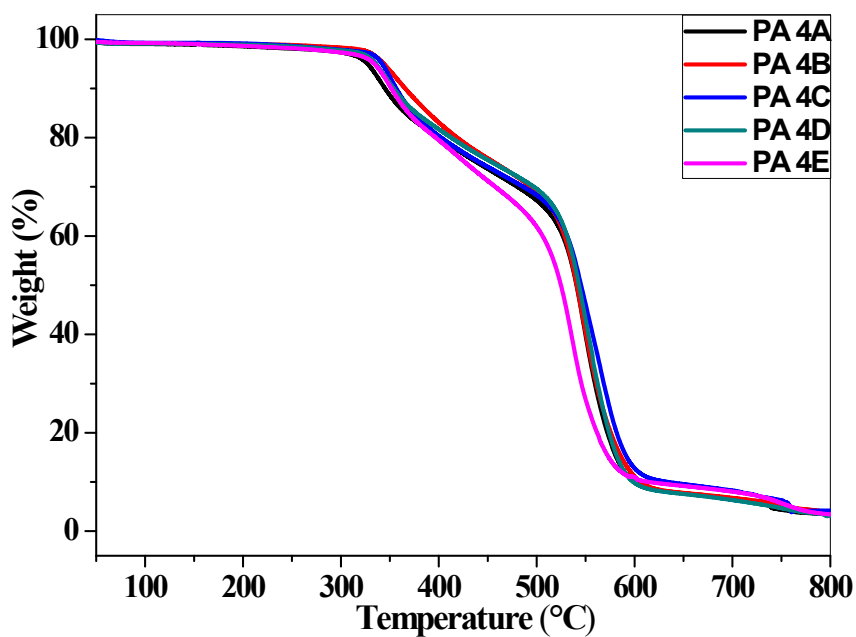


Fig. S3. TGA thermograms of the polyamides in air (heating rate: 10 °C min⁻¹).

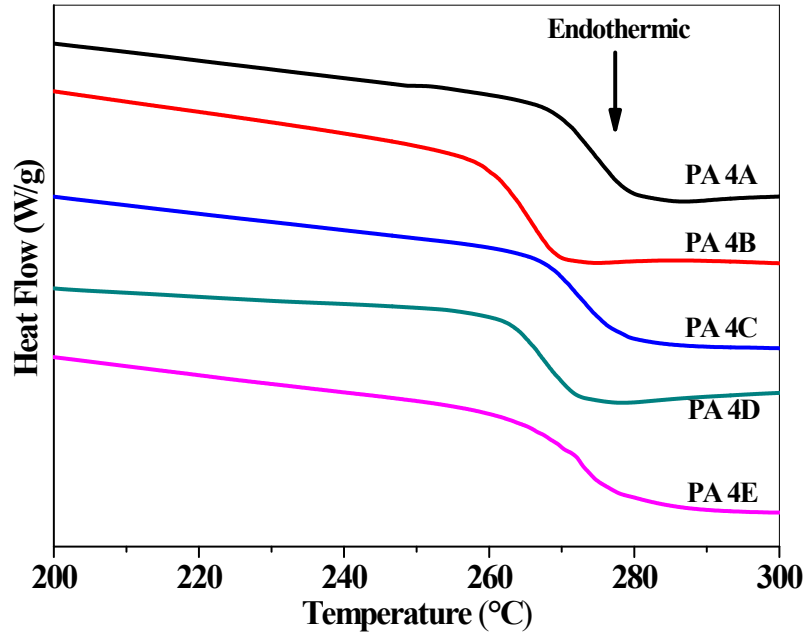


Fig. S4. DSC curves (2nd heat scan) of the polyamides (heating rate: 20 °C min⁻¹).

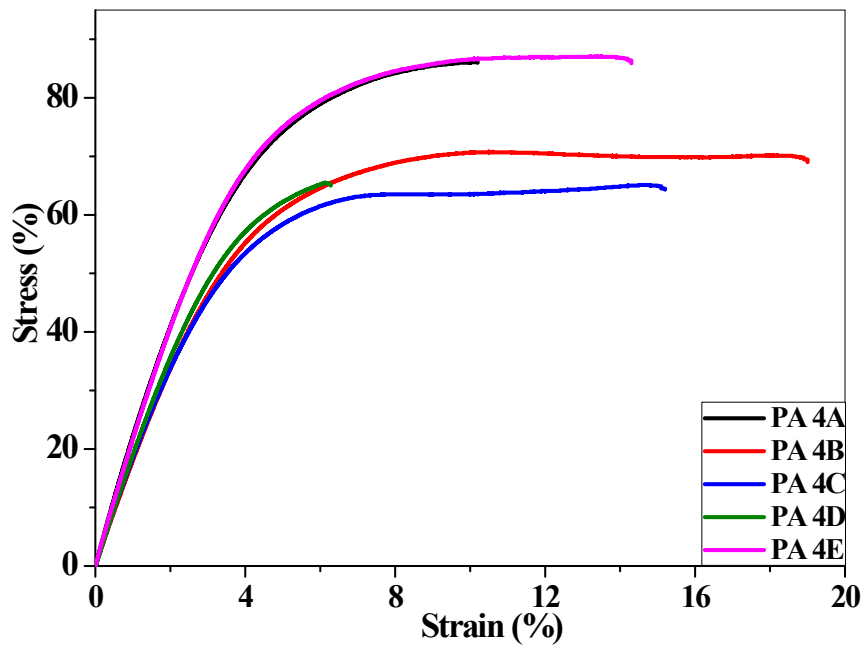


Fig. S5. Stress-strain plot of PA membranes.

Gas permeability vs. dielectric constant

Dielectric constant (ϵ) depends on molar polarization and molar volume of the polymer. Higher ϵ indicates higher cohesive forces, denser chain packing and lower FFV

in the polymer.^{4,5} It is observed from **Fig. S6.** that gas permeability has a relationship with the ϵ .⁶ The order of ϵ was PA 4A < PA 4B ~ PA 4C < PA 4E < PA 4D.

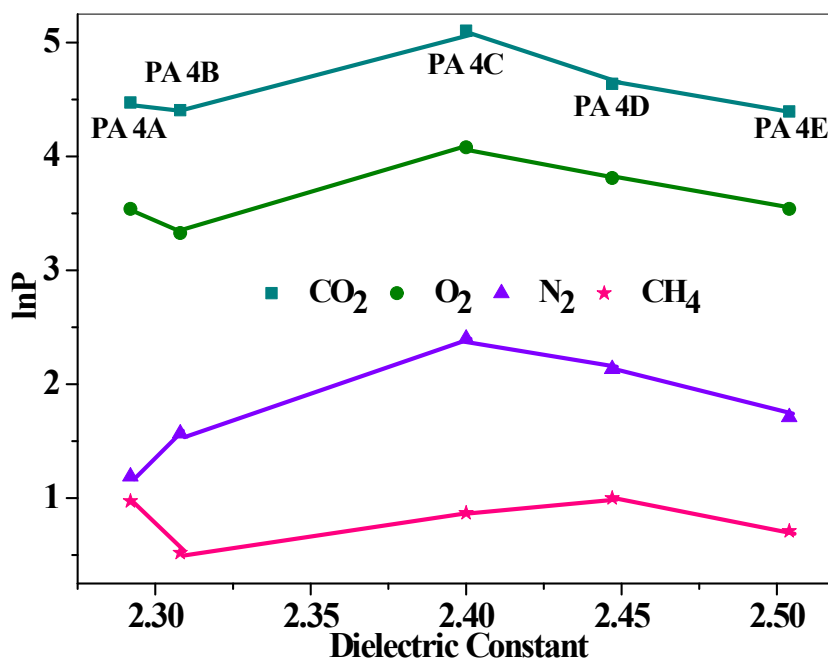


Fig. S6. The dependence of gas permeability vs. dielectric constant of the polyamide membranes for CO₂, O₂, N₂ and CH₄ gases.

References

- 1 S. Maji and S. Banerjee, *J. Memb. Sci.*, 2010, **360**, 380–388.
- 2 S. Bisoi, P. Bandyopadhyay, D. Bera and S. Banerjee, *Eur. Polym. J.*, 2015, **66**, 419–428.
- 3 E. M. Maya, I. García-Yoldi, a. E. Lozano, J. G. de la Campa and J. de Abajo, *Macromolecules*, 2011, **44**, 2780–2790.
- 4 S. Bisoi, A. K. Mandal, V. Padmanabhan and S. Banerjee, *J. Memb. Sci.*, 2017, **522**, 77–90.
- 5 D. Bera, V. Padmanabhan and S. Banerjee, *Macromolecules*, 2015, **48**, 4541–4554.
- 6 P. Bandyopadhyay and S. Banerjee, *Eur. Polym. J.*, 2015, **69**, 140–155.